THE PENNSYLVANIA STATE UNIVERSITY
SCHREYER HONORS COLLEGE

DEPARTMENT OF MECHANICAL AND NUCLEAR ENGINEERING

# A COMBINED APPROACH TO LOCALIZATION FOR A NUCLEAR CASK INSPECTION ROBOT

JACOB BECK
SPRING 2016

A thesis
submitted in partial fulfillment
of the requirements
for a baccalaureate degree
in Mechanical Engineering
with honors in Mechanical Engineering

Reviewed and approved* by the following:

Sean Brennan
Associate Professor of Mechanical Engineering
Thesis Supervisor

Zoubeida Ounaies
Professor of Mechanical Engineering
Honors Adviser

* Signatures are on file in the Schreyer Honors College.

## ABSTRACT

As part of an initiative to develop methods to certify and confirm the integrity of nuclear waste storage casks, a team of researchers lead by Penn State is working to create an inspection robot to inspect dry-storage casks. This thesis focuses on the development of localization technologies that can be used inside the casks. The interior of these casks is accessible via narrow cooling channels, which present a low-feature, high-temperature and high-radiation environment. The work in this thesis explores various localization methods, develops visual simulations of the cask internals, evaluates identified methods using those simulations, and finally constructs and tests a hardware prototype of the localization system in a physical mock-up. We show that selected computer vision methods utilizing lasers and edge detection perform well in simulation, and could be applied for real-world localization with further work.

# TABLE OF CONTENTS

# ACRONYMS AND ABBREVIATIONS

| | |
|---|---|
| BDL | Borehole Deployable Laser |
| DCSS | Dry Cask Storage System |
| ELF-EP | Extremely-Low-Frequency Electromagnetic Pulse |
| ICP | Iterative Closest Point |
| MPC | Multi-Purpose Canister |
| RMS | Root Mean Square |
| ROS | Robot Operating System |
| SCC | Stress Corrosion Cracking |
| SMR | Subterranean Mobile Robot |

## LIST OF FIGURES

## LIST OF TABLES

## ACKNOWLEDGEMENTS

First, obvious thanks should go to my thesis readers. I thank Prof. Sean Brennan, who went beyond the duties expected of thesis advisor to provide me with advice on a diverse range of topics, and with who I have enjoyed some of the most interesting classes I have taken as an undergraduate. Thanks also go to my second reader and honors advisor, Prof. Zoubeida Ounaies, who, despite her frequent traveling, always found the time to answer my questions.

I thank Prof. Cliff Lissenden, who first involved me in this project during an REU in the summer of 2014. I will always remember that summer as the pivotal point in my life when I decided I wanted to become a researcher.

Bobby Leary is deserving of thanks as my stalwart companion in research, whose practical experience in the lab and intense discourse in meetings brought out my best. Bobby was always willing to help me with implementation details, to provide a second opinion of my approach.

Finally, I would like to thank Kelilah Wolkowicz, for her help on my path to higher education, and without whom I would surely still be searching the lab for parts!

# Chapter 1

## Introduction

Within a nuclear power plant, there is a minimum temperature required of the fuel rods for efficient energy generation. Once fuel rods drop below this minimum temperature, they are removed from the reactor core. While this fuel is no longer considered useful for power generation, it is still very hot and radioactive. During the dawn of the nuclear age, experts developed a common plan for processing the national stockpile of nuclear waste. First, the waste cools in wet storage, typically within large, on-site pools of water. After an average of about 10 years [1], the fuel is cool enough to move into dry storage casks: large concrete and steel structures. The fuel is then stored in these casks until it can be transported to a national permanent storage site. In 1987, the Nuclear Waste Policy act was signed into law, allowing work to begin on such a site: the Yucca Mountain nuclear waste repository. However, in 2009, funding for further development of this site was largely reduced, effectively cancelling the project [2]. Currently, there are no plans to resume construction, nor funding to characterize any other sites. The ramifications of this are that dry storage, once intended only as a temporary measure, is now assumed to be the effective end of this waste stream, at least while alternative repository and processing options are being debated.

In order to use Dry Cask Storage Systems (DCSSs) for long-term storage, a re-certification process may benefit from inspection methods to verify the continued integrity of the

casks over an extended period. Unfortunately, there are limited technology options to perform non-destructive inspection of dry storage cask systems. This thesis focuses on the development of some of these technologies.

A typical dry storage cask consists of two major components: an inner Multi-Purpose Canister (MPC) that holds fuel, and an outer overpack. Between these two components is ventilation space, to convect heat away from the canister.

This thesis will focus specifically on the Holtec HI-STORM family of dry-storage casks, as it is one of the more common DCSSs in use today [3]. The inner canister of a HI-STORM consists of welded stainless steel, and rests within an overpack of steel-clad concrete. Once the cask enters service, the canister is carefully filled with spent fuel rods, welded shut, and then backfilled with inert gas. Finally, the canister is lowered into the overpack, and a lid is affixed. A cut-away schematic showing the components of a HI-STORM 100 is shown in Figure 1.

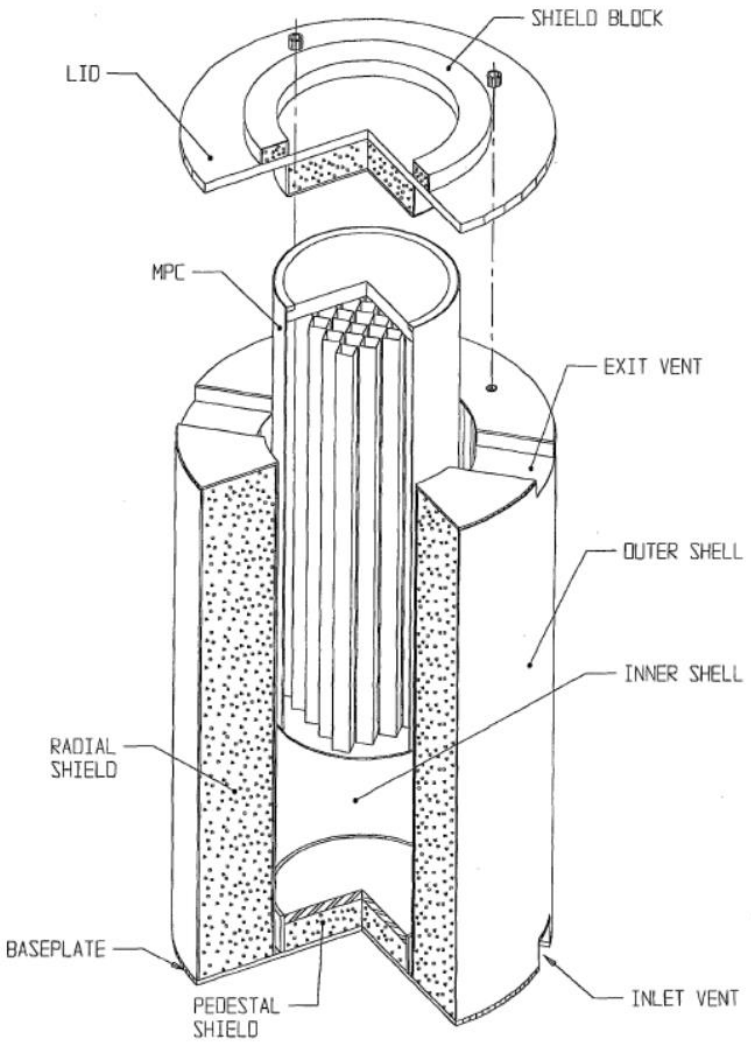


**Figure 1: Exploded view of a Holtec International HI-STORM 100 storage system [4]**

There have been no known in-use failures of storage canisters, and to continue this unblemished record, expert knowledge must infer modes by which storage casks might fail under any possible scenarios. The most likely failure scenarios, according to experts, include Stress Corrosion Cracking (SCC) [5] and concrete degradation [6]. SSC refers to the process where chemical attack combined with residual stress from the manufacturing process can lead to the development of hairline fractures in a weld-affected zone. In a typical cask, the canister is

fabricated by welding rolled stainless steel, which introduces the residual stress at the welding site. As air circulates around the cask, it may deposit chlorine from salts, and even other chemicals dissolved in atmospheric moisture onto the canister surface. If combined deposition and stress conditions are met, cracking of the canister may initiate, which if left unmitigated for a long enough duration, risks exposing radioactive material to the environment. Similar physical processes may lead to the degradation of concrete by decalcification and sulfate attack [7], and extended exposure to high temperatures have been shown to weaken concrete [6]. These processes may result in a weakening of the outer cask structure. Furthermore, there are instances of concrete used in casks developing cracks from moisture expansion during freeze-thaw cycles [8].

An effective inspection strategy must determine if the failure-possible environmental conditions are present within the cask. If damage is measureable, then another goal is to estimate the extent of damage. Current inspection methods are mainly visual, using borescopes in conjunction with temperature probes [9]. These actions alone are insufficient for detecting the hairline cracks and chemical conditions associated with SCC and concrete degradation.

With these goals in mind, researchers at The Pennsylvania State University organized a project to develop a robotic inspection system with the goal of developing processes and techniques to re-certify storage casks [10]. The robot should traverse the cooling channels within the overpack and thereby take measurements for characterization using a variety of sensors. One of the challenges to the development of this robot is the extreme conditions that may be present inside the cask, requiring the use of robust hardware. Temperature and radiation conditions vary widely with age of the stored fuel and location within the cask. Some worst-case values are estimated to be 205°C for newly loaded fuel, and $2.71 \times 10^4$ rad/hr activity after 5 years [5]. A

major facet of this project is the development of robot-supported sensors that can collect useful data and operate under these harsh conditions.

As part of the inspection process, the robot must be able to accurately determine its position within the cask. This is essential for locating trouble sites, correlating sensor data with position, and revisiting areas of concern during follow-up inspections. The design of the cask is particularly troublesome in this aspect, as it contains homogenous surfaces, tight confines, and attenuating materials. These troublesome aspects largely rule out or reduce the effectiveness of popular robot localization methods.

With these considerations in mind, this thesis investigates the use of visual navigation and inspection techniques. Cameras are already required sensors for the robot to perform visual inspection, and so using optical methods does not require any additional hardware. One of the advantages of applying visual techniques to this problem is that the interior of the cask is pitch black, which would normally pose an issue, but in this case means that we will have complete control of the lighting conditions. Because of this, our research focuses on how lighting can be used to enhance visual techniques, and how the data from these methods can be used to localize.

We have already discussed our focus on the HI-STORM 100 model of cask, but we will further constrain the problem by primarily considering movement within the ventilation channels around the circumference of the canister. These channels are defined by the inner surface of the overpack, the outer surface of the canister, and rails which form the sides and serve to center the canister (see Figure 2). These vertical ventilation channels are narrow and long, and due to curvature (see Figure 3), constrain a rectangle with dimensions of roughly 7.44” wide and 1.81” high [11]. The height is slightly variable, as it depends on how well the canister is centered within the overpack. The overpack surface is of high concern for inspection, as the curved outer

surface of the canister is at the highest risk of developing SCC. Because the channels are relatively narrow and restrict motion, we are primarily concerned with longitudinal motion, but an effective localization strategy should fully define the robot position in all degrees of freedom.

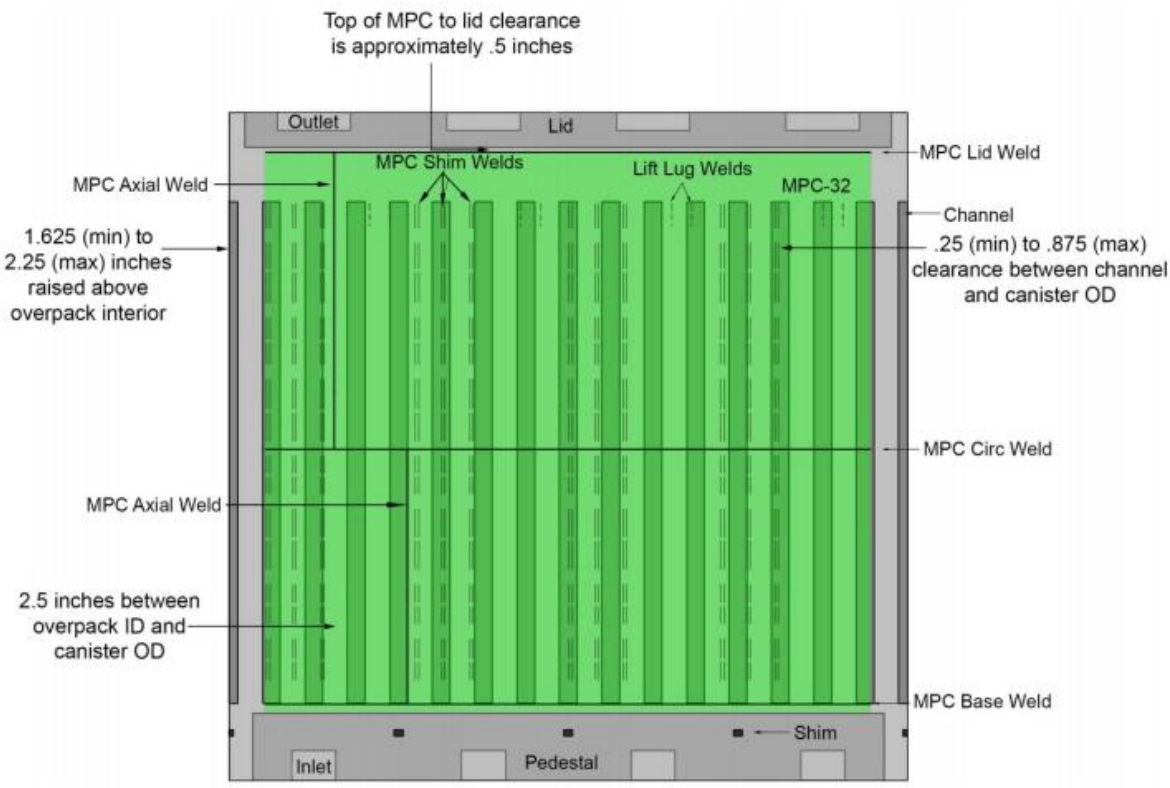


**Figure 2: Unrolled view of the air gap between the MPC and overpack [5]**

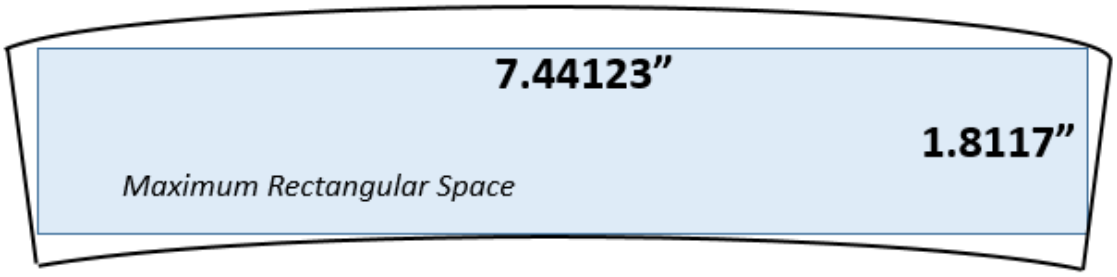


**Figure 3: Rectangle as constrained by channel dimensions [11]**

The conceptual design of the inspection robot is that it is inserted into the vertical channel using a large arm that rests on the top of the canister. The robot itself consists of one or more inspection cars which are lowered from the end of the arm via a winch into the channels. The goal of this design approach is to locate nearly all actuation components out of the narrow confines of the channel and either outside of the case or onto the top surface. This allows the inspection cars to act almost wholly as carriers for the sensors. Figure 4 shows a drawing of this concept robot within the cask prior to entry into the vertical air gap, which is to the bottom left of the robot in this figure.

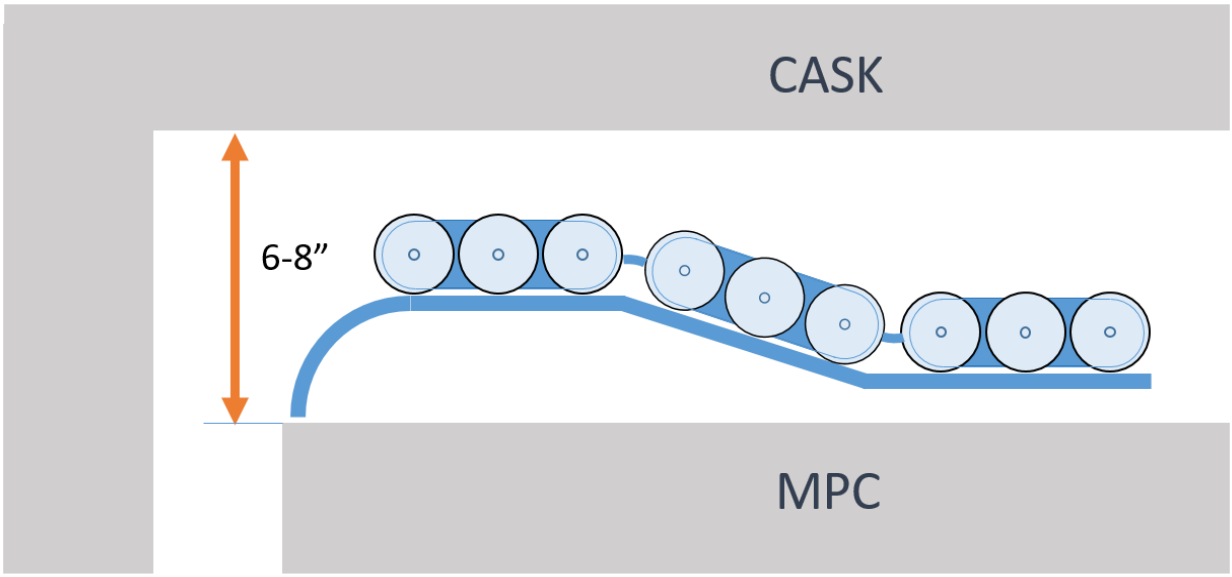


**Figure 4: Concept of the inspection robot resting on top the MPC [11]**

# Chapter 2

## Literature Review of Localization Approaches

### General Inspection Robots

To our knowledge, the ventilation channels of the cask impose tighter than usual constraints on the size and cooling of our robot than usually encountered in nuclear inspection. The majority of nuclear inspection robots are designed to investigate the nuclear plant itself, and so are generally larger. To this end, we focus specifically on robots designed to inspect small-space and/or low feature environments.

We begin our review with a robot designed to explore steam chests, an environment similar in material and appearance to DCSSs. Tache et al. developed this robot, which they call MagneBike, named for its bicycle style design. The MagneBike provides an interesting case study, as it is one of the few inspection robots to attempt localization in full 3D. Steam chests as an environment are similar to nuclear storage casks in that they are constrained, dark, and metallic. However, unlike storage casks, they have a complex 3D interior structure. The MagneBike, the design of which can be seen in Figure 5, posses large (relative to the body) magnetic wheels that allow it to climb inside the pipe network within these chests. Because of the complex 3D shape of the target environment, the MagneBike must have robust methods to accurately determine its location within space for effective inspection. In order to achieve this,

Tache et al. fuse data from wheel encoders with an accelerometer to calculate 3D odometry. A map is generated from 3D laser scans, which are periodically matched using Iterative Closest Point (ICP) to correct drift in the odometry predictions [12].

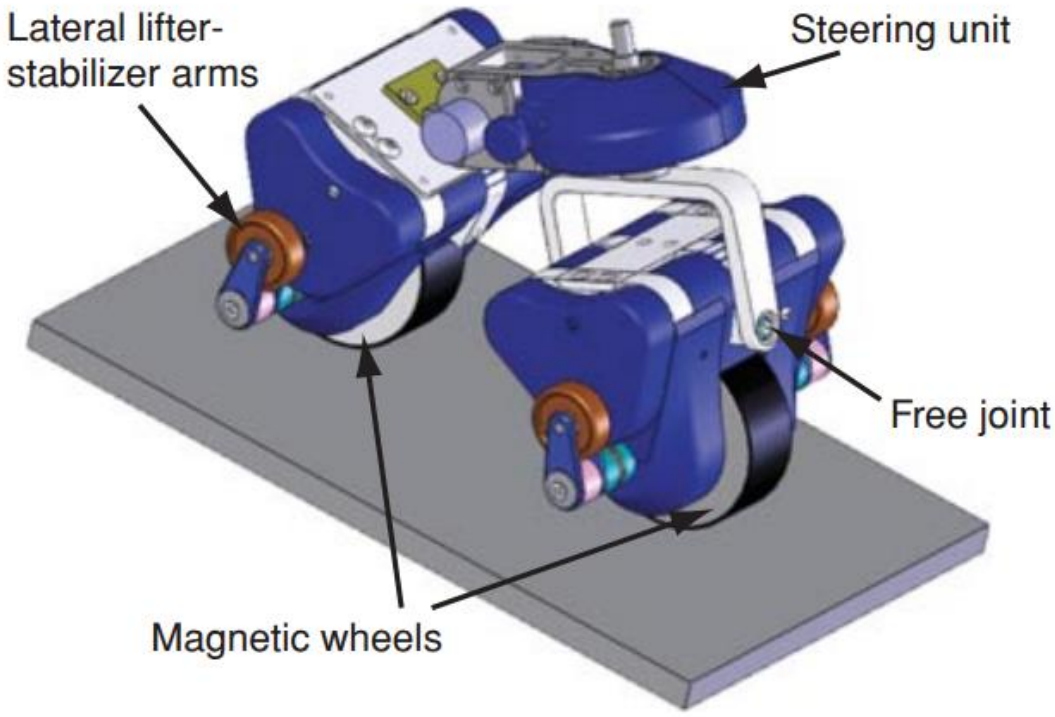


**Figure 5: Design of the MagneBike inspection robot [12]**

Outside the nuclear industry, development of the sewer pipe inspection robot KANTARO is heavily documented by Nassiraei et al. The most unique feature of KANTARO is its passive steering system, which allows it to naturally follow the curvature of pipe networks without operator input. Localization is performed by a combination of odometry and laser scans. As can be seen in Figure 6, the laser scanner is mounted on the end of the robot, so that it takes a radial scan of the pipe. As the robot drives through the sewer, the laser traces forms a spiral along the pipe surface. This laser range data is fused with odometry readings to form a map of the interior of the sewer system, which is compared to official schematics. The pipes sections are generally

uniform and therefore provide no useful information for odometry correction, so comparisons are made between the distances of more apparent features (drains, plumbing intersections, man holes, etc.) [13] [14].

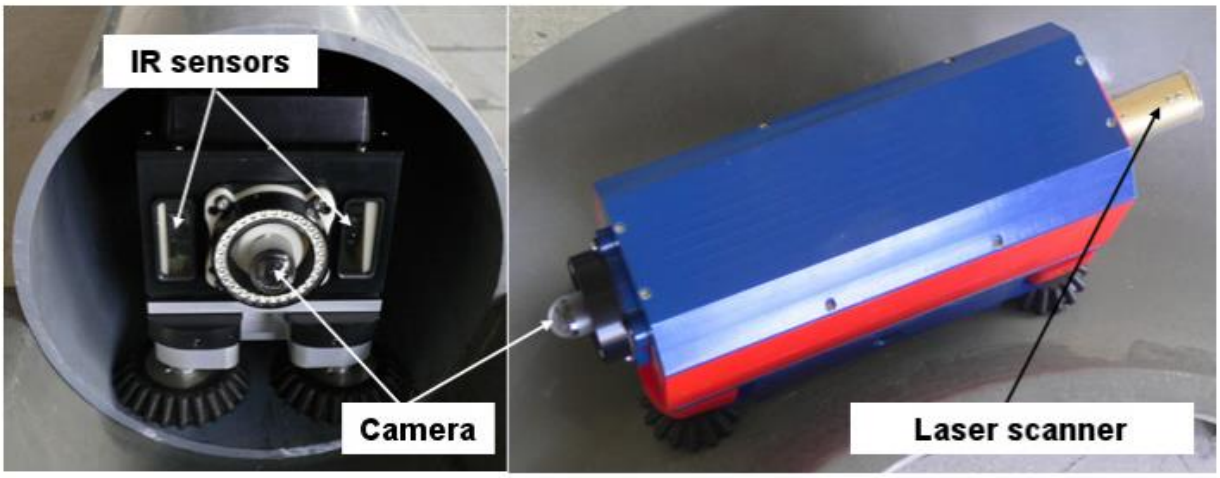


**Figure 6: The KANTARO sewer inspection robot [14]**

Morris et al. provide an overview of various robots designed for mine exploration, broadly classifying platforms by borehole or portal access, submersible/dry, and ability/lack of ability for locomotion. Borehole access is of particular interest to us, as the challenges of borehole exploration are similar to those of cask inspection: narrow, dark spaces that preclude the use of radio. One classification of robots discussed is Borehole Deployable Lasers (BDLs), cylindrical devices designed to be lowered into a cavern by way of a borehole, and take laser scans of the structure [15]. Figure 7 illustrates this process.

The other type of robot of interest to this project are the Subterranean Mobile Robots (SMRs), for their sensing and navigation techniques. The SMRs presented are shown in Figure 8. They are robust and slow-moving, such that any control algorithms may ignore any dynamics.

For sensing, they are equipped with gas sensors for methane detection, float switches for standing water, and laser scanners and IMUs for navigation.

**Figure 7: The process of using a BDL for void inspection [15]**

**Figure 8: Groundhog (left) and Cave Crawler (right), two SMRs [15]**

While the designs presented are proven to be effective, it is apparent that they all rely on laser scanners to sense the environment. Unfortunately, in the cask inspection application, we

cannot mimic this approach as, to our knowledge, there are no LIDAR devices commercially available which are compact enough to be used in our target environment. However, as we will discuss later, lasers are not the only technology that can be used to acquire dense point clouds, and the core concept of accurate localization is the fusion of information. To that end, it may be possible for us to record odometric measurements from our inspection robot either by tracking the rotation of a free wheel along the channel wall, or from an encoder embedded within the winch of the arm. However, these devices will only provide us with a total distance, and cannot be used to measure lateral movement or rotation within the channel, necessitating additional sources of information.

**Unconventional Sensing Techniques**

It can be observed from our review of inspection robots that many depend on a combination of odometry and lasers scans for localization. As previously discussed, there are no LIDAR units suitable for our application, and so a focused search for other localization technologies was performed.

Realizing that radio-based techniques have poor penetration of soil, Markham et al. develop a technique to perform subterranean tracking of wildlife using low-frequency magnetic fields. The system consists of a collection of transmitting coils placed in known locations above ground, and remote detector coils on a tracking collar (see Figure 9). The transmitting coils are energized in sequence, and are modulated (at a low-enough frequency for the magnetic field to be considered quasi-static) to transmit a message encapsulating the antenna ID and a timestamp,

which are recorded along with the signal strength by the collar. When the animal leaves the tunnel system at night, the collar uploads the recorded data to a monitoring computer over a conventional radio link. The data is later collected, and a particle filter processes the data to determine location based on the signal strength from each transmitter and their known layout. Markham et al. report a 3D RMS error of 0.45m, but note a reduction in accuracy when ferrous objects are present [16].

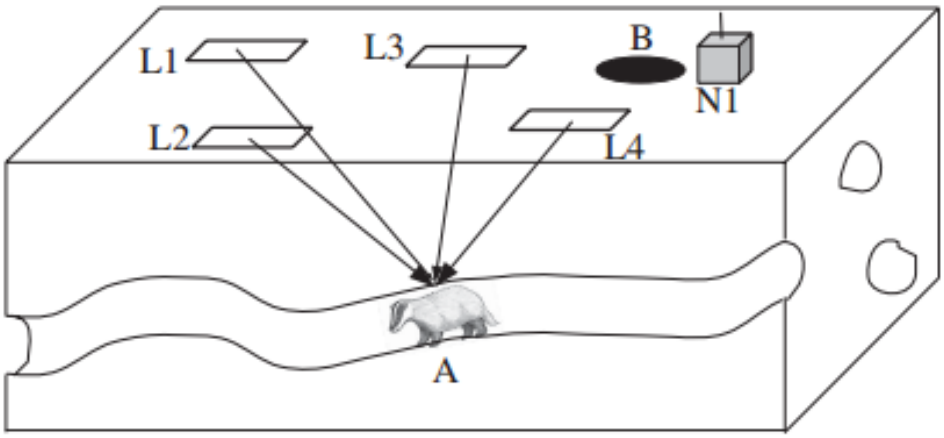


**Figure 9: A magneto-inductive tracking system showing transmitters (L1-L4), receiver (A), and a basestation (N1) near the tunnel exit (B) [16]**

Facing a problem similar to that in this thesis, Qi et al. develop a radio system for communication and localization of a pipeline inspection robot. This system is designed specifically to deal with the issues of radio propagation through metallic pipes, by using periodic Extremely-Low-Frequency Electromagnetic Pulses (ELF-EPs). By using an emitter that creates a signal with two large lobes and an array of sensors (as illustrated in Figure 10), the position of the robot along the length of the pipe can be determined from the relative signal strength at each receiver. In practical tests, Qi et al. report their system achieves errors typically less than 0.45m [17].

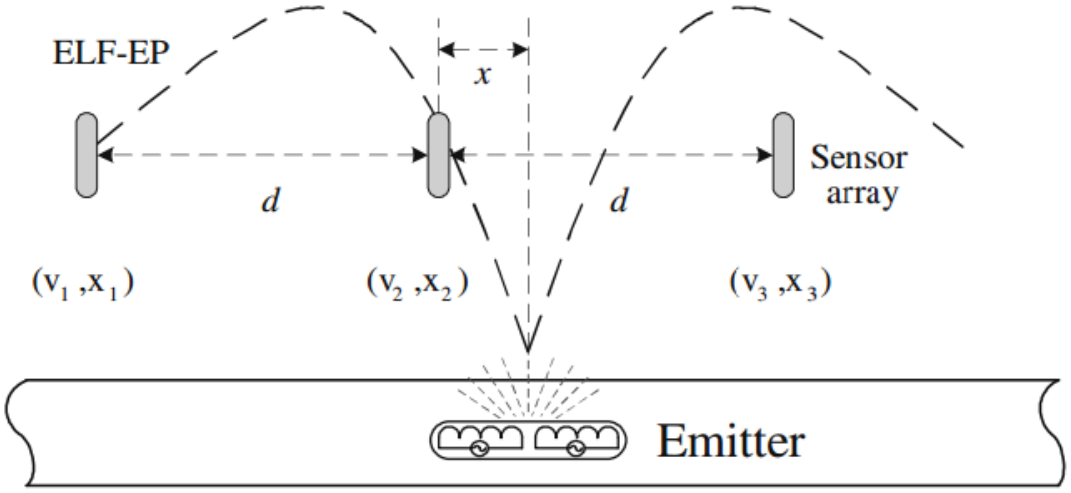


**Figure 10: Localization by measuring the strength of ELF pulses [17]**

The first system described presents an intriguing method of localization, but as noted, it loses accuracy in the presence of ferrous material. This renders it unsuitable for our application, as the cask is steel-clad. It may be possible to model the interactions between the cask and an applied magnetic field in order to account for the distortion, but such analysis is outside the scope of this thesis. The second system is interesting, as the data required for localization is collected by external equipment as would be the situation in this study. However, the implementation detailed is 1D only, and both methods described provide accuracy of only approximately 0.45m; this is sufficient for large-scale pipes and sprawling burrows, but insufficient for our relatively small channel.

**Computer-Vision Based Techniques**

Thus far we have effectively ruled out the use of LIDAR and radio-based techniques, leaving computer vision for mapping and navigation. As discussed previously, our robot already requires cameras, and so, in general, optical techniques will not require any additional hardware. A drawback of many of these techniques is a high computational cost, but this processing can be performed off-board the robot. The main difficulty faced in implementing visual methods to our application is the lack of distinct visual features within the cask, which consists mainly of very homogenous surfaces, specifically polished stainless steel. For this reason, we reviewed techniques devised to overcome this.

Stereo vision is perhaps the one of the most common sensing methods for robots. However, stereo depends on the ability to pick features out of each image and match them to the other, and as mentioned, our environment is feature-deprived. A simple technique to enhance the captured images with more features is texture projection, where a light pattern is projected on to the physical scene. The cameras then capture this scene, which now appears to have texture on each surface. The improvement in matching from this texture is illustrated by the disparity maps in Figure 11. By creating and analyzing a model of the camera-projector system that considers the effects of pixelization and blurring, Konolige attempts to create an optimal texture pattern for projection [18]. Leeper et al. apply this concept to integrate a compact stereo camera system onto a gripper for improved close-range grasping performance. They perform no optimization of the projected texture, and claim that even a simple grid of dots created from a compact laser can improve the quality of stereo matching [19].

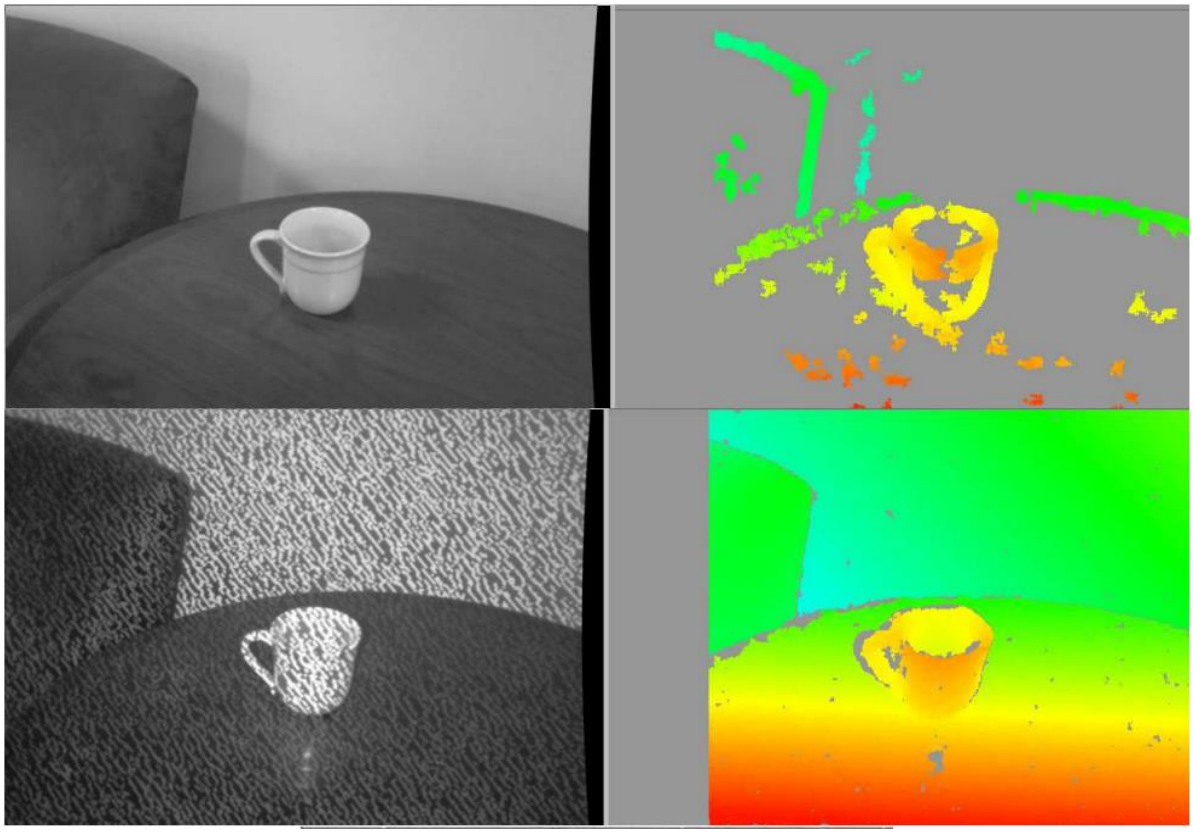

**Figure 11: Scene and disparity map under normal conditions (top), and with projected texture (bottom) [18]**

Careful control of lighting to enhance visual techniques is not a new concept, and is studied under the name of structured lighting [18] [20]. Similar to how stereo vision uses the disparity in separate images to calculate depth, structured lighting uses a single camera and projector to observe the deformation of a known light pattern to infer details about the environment.

Zhang et al. review the basic principles of structured light, and apply those principles to design a system for inspecting the internal surfaces of pipes and other tubular structures. The system, as illustrated in Figure 12, consists of a laser directed at a camera with an attached reflector. The laser bounces off the reflector and forms a ring of light on the interior surface of the pipe. The camera observes the light to determine the profile of the pipe, translating down the

length of the pipe to develop a scan of the entire interior. In physical tests, Zhang et al. report a worst-case RMS error of 0.041mm [20].

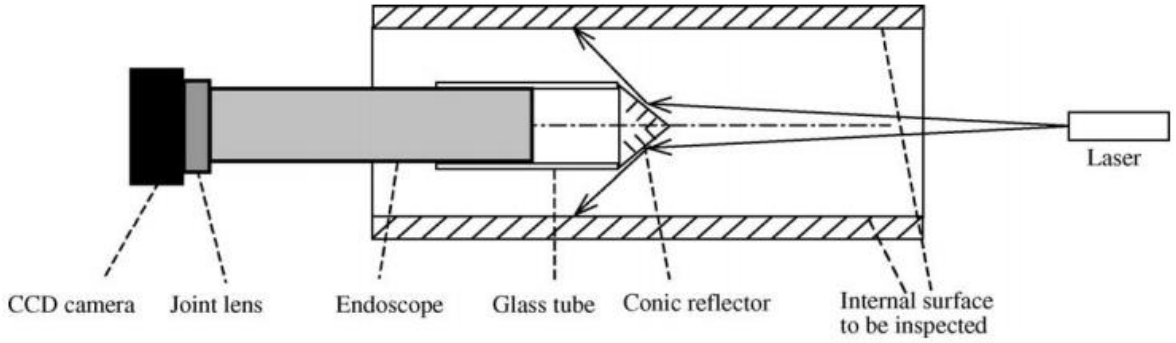


**Figure 12: A system for inspecting pipe interiors using circle structured light [20]**

Beyond the modeling of patterns required for structured light systems, Martin describes how just careful selection of light source and location can drastically improve the quality of camera images for thresholding and other vision algorithms [21]. Figure 13 shows how just a simple filter can make desired visual features much clearer.

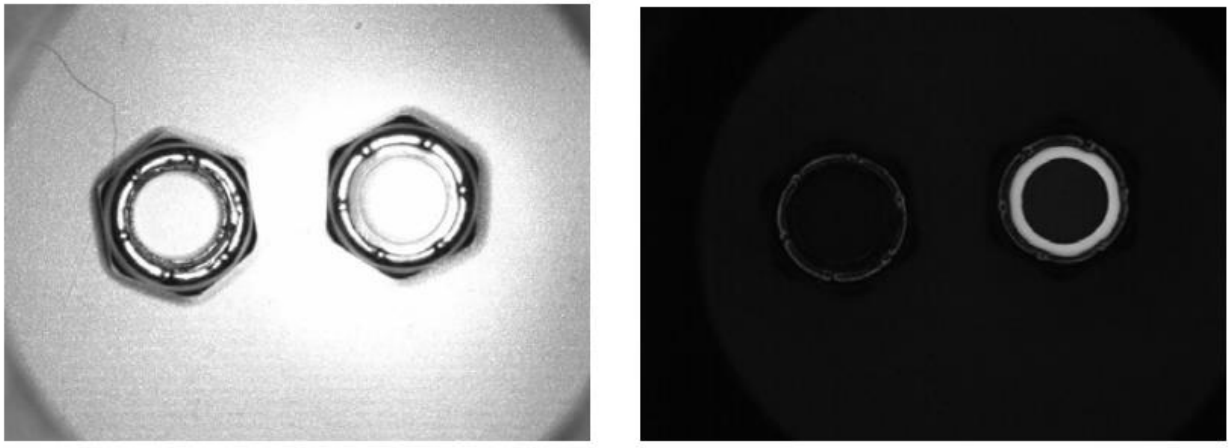

**Figure 13: A red (>510nm) filter blocks ambient light (right), showing the UV reflected by the nylon ring [21]**

The final class of visual methods we would like to review are more “traditional”, in that they have no special interaction with the lighting source. One of these methods is visual

odometry, which tracks the movement of features through the image to estimate ego-motion. Hansen et al. present development of an algorithm to localize by measuring the movement of corrosion patterns on the interior of a pipe. By applying the known diameter of the pipe in question, they are able to resolve the scale ambiguity associated with monocular vision. In addition, they use this odometric data to stitch imagery and form appearance maps such the one shown in Figure 14 [22].

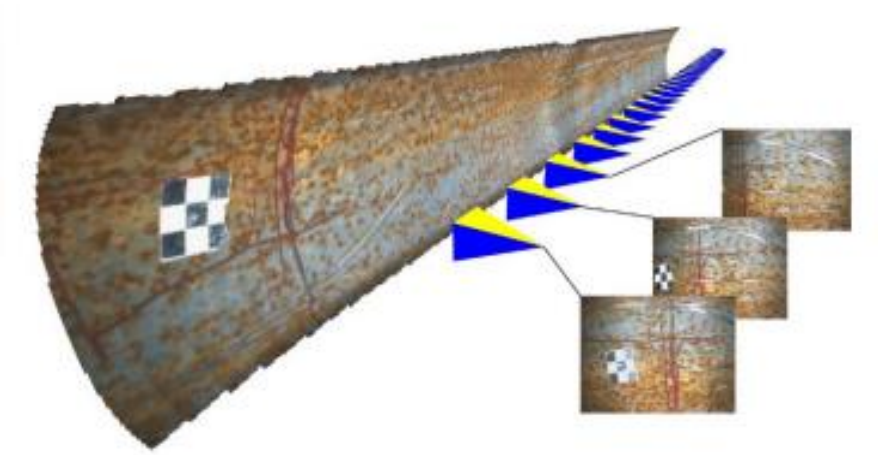

**Figure 14: Render of pipe interior created from camera imagery and odometric data [22]**

In addition to providing data useful for localization, De Paz et al. present a technique directly applicable to inspection: crack detection. De Paz et al. note that one of the most common problems with image thresholding is the variability associated with different lighting conditions. To overcome this, they perform several operations on the image, including logarithmic transformation of intensity, subtraction of the known illumination pattern from the lighting system, and a wavelet transform. After these processes, thresholding is applied using Otsu's method, resulting in the image shown in Figure 15 [23].

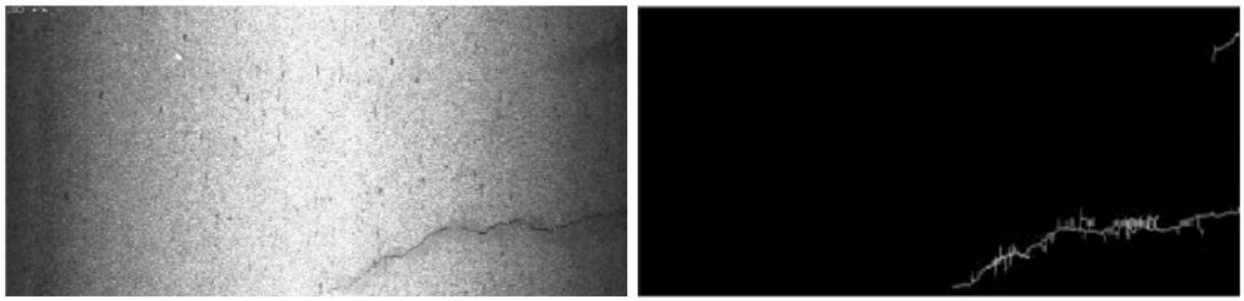

**Figure 15: Original grayscale image with crack (left), and binary image after processing (right) [23]**

Comparing the visual methods presented, projected texture seems to be a simple to implement and effective sensing technique, and so we select it for further investigation. The high precision of the structured light technique described by Zhang et al. could be used to capture features for localization, but as the investigators note, this would require development of projection system integrated with the camera assembly, such that it can be inserted into blind holes. Visual odometry could be used to directly measure movement; however, unlike Hansen et al., our environment lacks apparent visual features. It may be possible to setup a close-range system to capture small surface features for tracking. While crack thresholding may seem at first ideal for our application, we expect the damage associated with SCC to either be microscopic and thus not visible, or not present at all.

# Chapter 3

## Simulated Environment

### Selection of Simulation Package

Having selected a variety of sensing and localization techniques to pursue, we next decided to develop a set of simulations with which to evaluate those techniques. Many software packages for robot simulation exist, each with various advantages and disadvantages. Having determined that the most promising techniques were vision algorithms, it was decided that, most importantly, a suitable simulation package must provide us with photorealistic renderings of the cask environment. This capability allows a simulated environment to be used for testing of vision-based guidance and mapping algorithms to determine how they respond to various lighting conditions, surfaces, imaging errors, etc.

Beyond visual quality, there are several other features desired from an ideal simulation system. The Robot Operating System (ROS) is a middleware commonly used for passing sensor data between programs and over networks, and the Brennan research group uses this software extensively. Since ROS will likely be used in the final robot architecture, a simulator that integrates with this middleware will greatly ease the transition from prototype to implementation. In the context of this thesis, we are mainly concerned with visuals; however, software capable of rigid- and soft-body physics simulations would also prove useful for additional work. Finally, there is the practical requirement that the simulator software should have little to no cost.

Given these requirements, the software packages shown in Table 1 were compared. The selected packages for comparison consisted of the rendering software Blender, the official ROS simulator Gazebo, general robotics simulators Morse and Webots, and the video game engine Unity.

**Table 1: Comparison of simulation packages**

| | **Blender** | **Gazebo** | **Morse** | **Unity** | **Webots** |
|---|---|---|---|---|---|
| **Physics engine** | Bullet | ODE, Bullet, Simbody, Dart | Bullet | PhysX | ODE |
| **Price** | Free | Free | Free | $1500 (for Pro) | $3500 (for Pro) |
| **ROS integration** | None | Full | Full | With plugin | Full |
| **Visual quality** | High | Low | Low | Medium | Low |

After examining the pros and cons of each package, the open-source rendering software Blender was selected for further development. Of the packages evaluated, it offered the most realistic renders, and had the most permissive license. Furthermore, despite not having any official ROS support, a work-around exists that enables Blender outputs to be saved to images and videos which can be played back over the ROS messaging system.

**Simplified Model**

For initial testing, we approximated the channel as a perfectly 189x46mm rectangular shape. A topic of some concern was the application of realistic textures and shaders to model in order to simulate the interaction of light as accurately as possible. We have observed that during assembly, the outer surface of the MPC is polished to a very fine, highly reflective finish. While a brand new cask may have interior surfaces like this, we do not know how casks that have been in service (in some cases for over 40 years) will weather. It is possible that the overpack will protect the channel, and it will maintain a near-factory finish, or it may become corroded, pitted, and/or covered with dust. With insufficient information to accurately model the channel walls, we opted for a moderately reflective finish and very fine texture that qualitatively appeared realistic, based on our observations of new casks at a Holtec assembly plant.

Noting that the robot itself will subtly influence the appearance of the environment, it was also modeled. At this stage, the robot was represented as a simple white prism with a set of cameras and a lamp/projector. An editor level view of this system is shown in Figure 16.

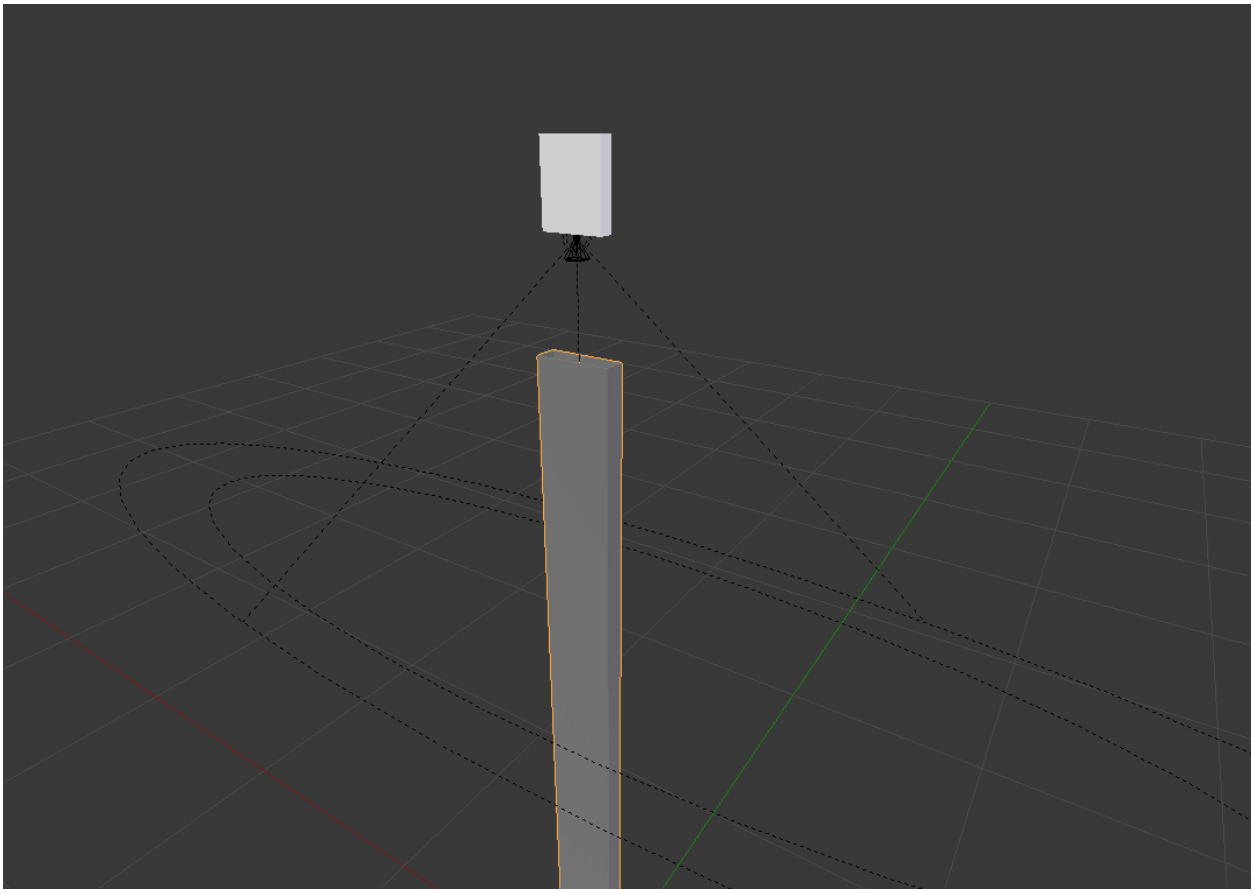

Figure 16: Unrendered view of robot and channel for basic simulation

## Complete Model

The simplified simulation model allows rapid testing, but not does capture the true geometry of the channel, various materials, and interactions from ambient lighting. For more realistic testing, we extended the basic simulation by replacing the simplified channel with a model of the cask based on engineering drawings. The MPC used the same stainless steel shader as the basic simulation, and the overpack appearance was based on the drab paint seen in photos

of storage sites. The robot model was unchanged from the basic version. An editor level view of this more realistic environment is shown in Figure 17.

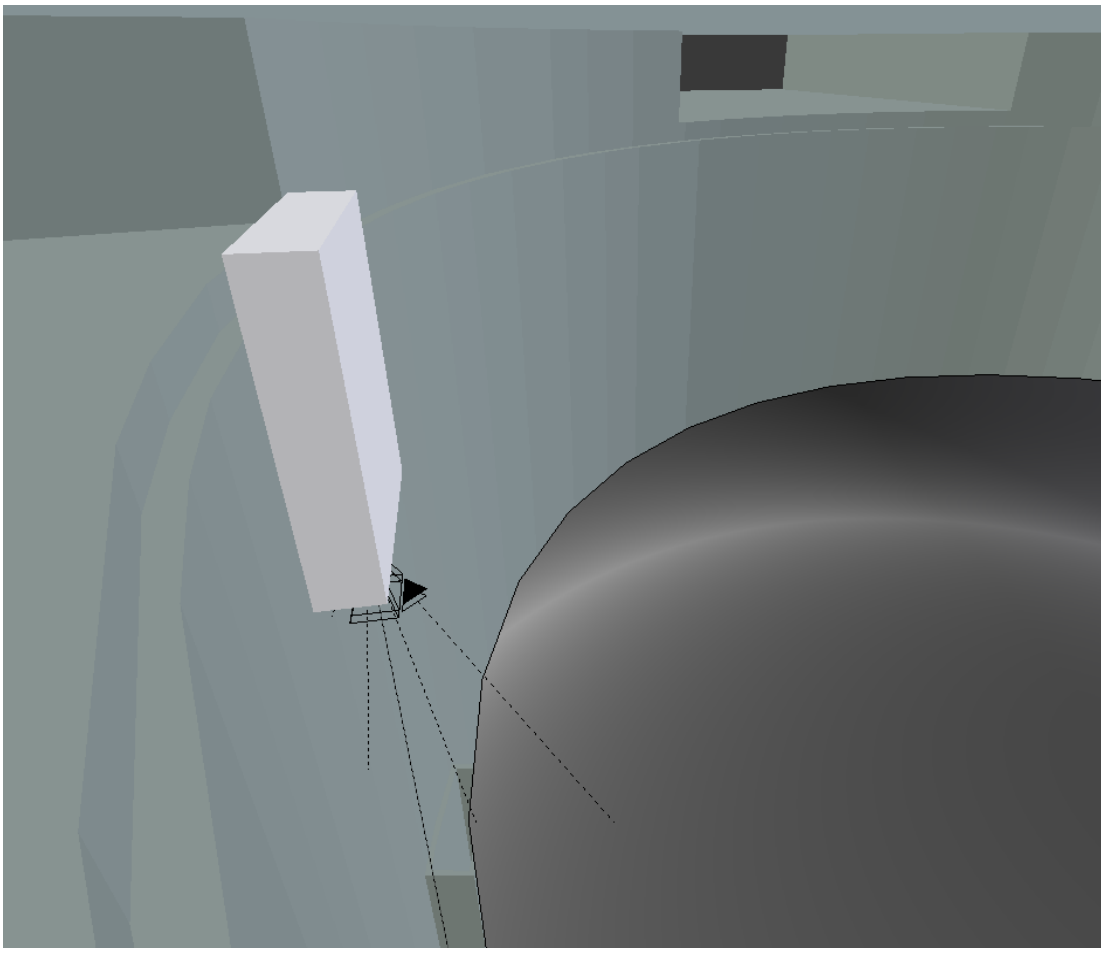

**Figure 17: Unrendered view of robot inside cask for comprehensive simulation**

The simulated environments presented allow us to rapidly test and evaluate visual feature extraction methods, without the need for investing the resources in a hardware implementation. Having designed these virtual test environments, we proceed to apply our selected visual methods on the rendered scenes.

# Chapter 4

# Feature Extraction

## Projected Texture Stereo

A dense point cloud represents a fantastic feature set to use for localization. The most typical device for producing one is a laser scanner, but as discussed, this is unsuitable for our target environment. Another common method to create point clouds is via stereo vision, which depends on the successful detection and matching of visual features. As the cask is visually sparse, this method alone might also be insufficient. However, by projecting light patterns on to the environment, we can artificially add features to the images, which may improve the quality of stereo matches.

To test the effectiveness of this projected texture technique, we simulated the projection of a laser grid on to the surfaces of the cask, as shown in Figure 18. Stereo images of this simulation were then rendered and processed with a simple block-matching stereo algorithm. The results of this testing with and without projected texture can be seen in Figure 19, which clearly shows an improvement in the quality of the disparity map.

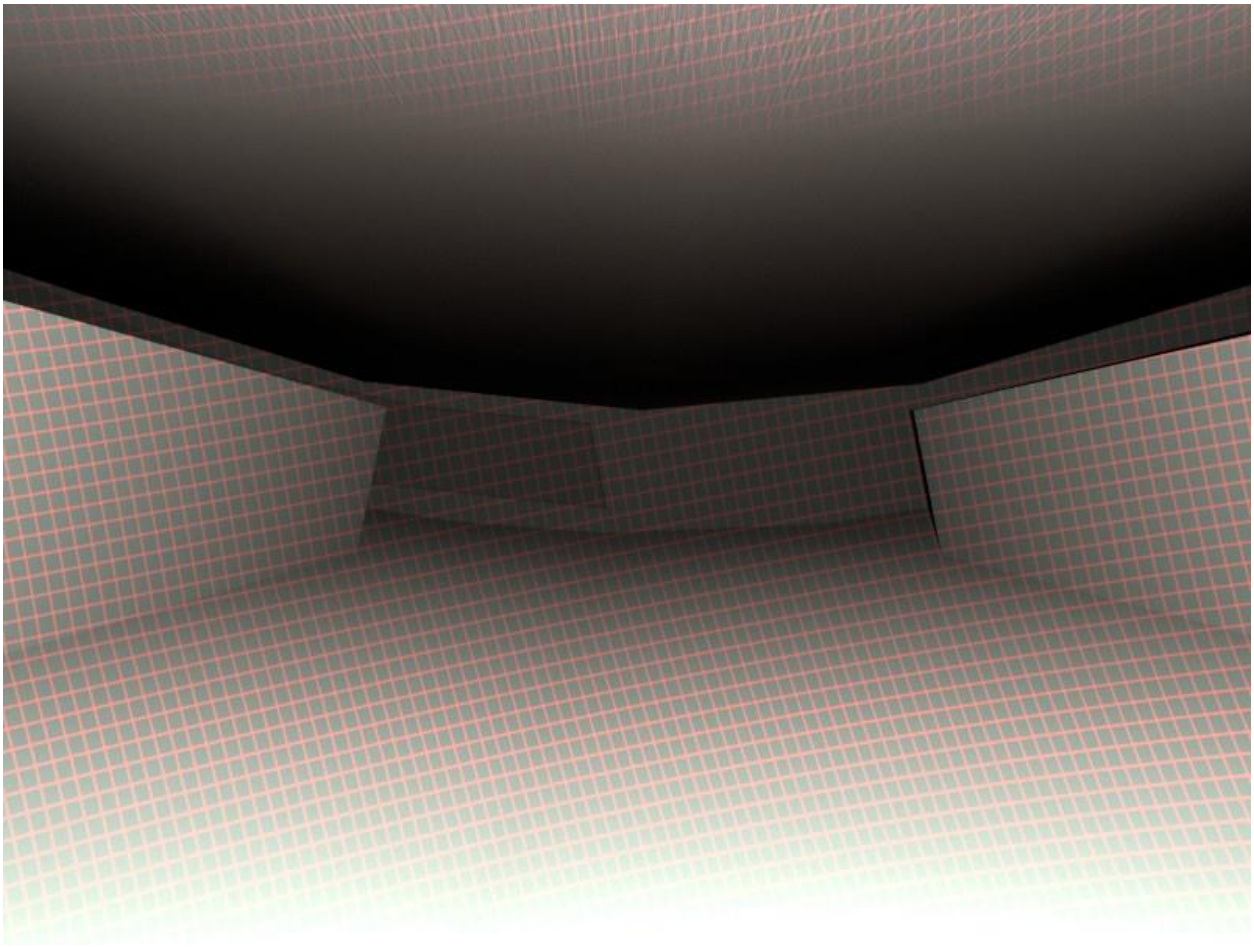

Figure 18: A grid pattern projected by a laser onto the simulated channel

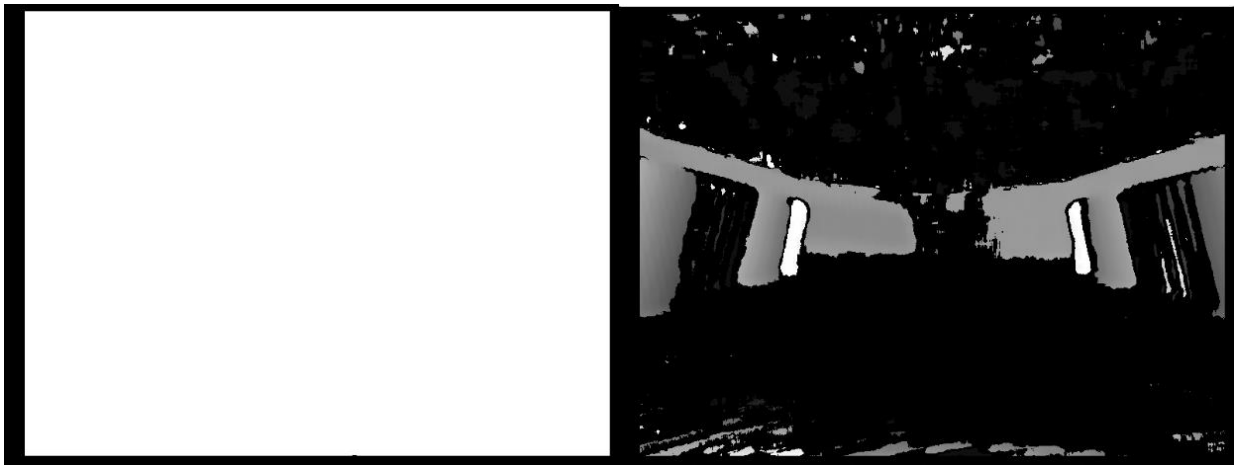

Figure 19: Disparity maps with (right) and without (left) laser-projected grid

## Corner Detection

Given the known dimensions of the channel, if we are able to detect known features, we can use our prior knowledge to resolve the scale ambiguity. Noting that in the simplified simulation, shadows that outline the corners of the channel would form, we chose to filter the image with a Harris corner detector. As shown in Figure 20, the detector was easily able to find these features, and so it would be possible to derive the homography matrix, which coupled with a known scale factor, would give us the associated transformation and rotation.

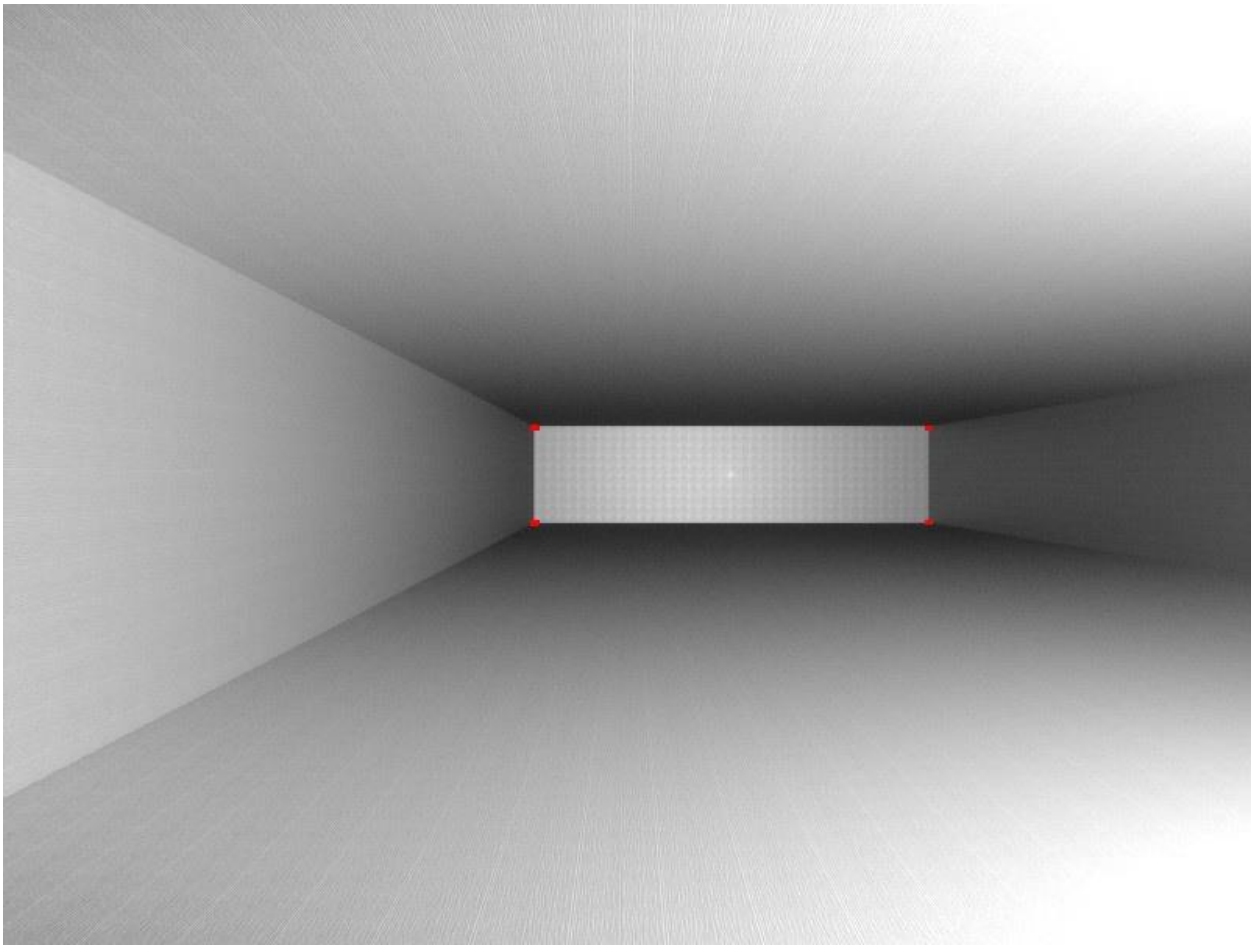

**Figure 20: Corner detection in simplified simulation**

Unfortunately, due to the different materials used in the more realistic simulation, these corners were less apparent (as seen in Figure 21). Another issue encountered was a lack of uniform illumination from the robot-mounted lamp. With fewer reflective surfaces, less light reached the bottom of the channel, leaving the end mostly in darkness. Increasing the output of the light source did lighten the environment, but the corners did not become any more apparent.

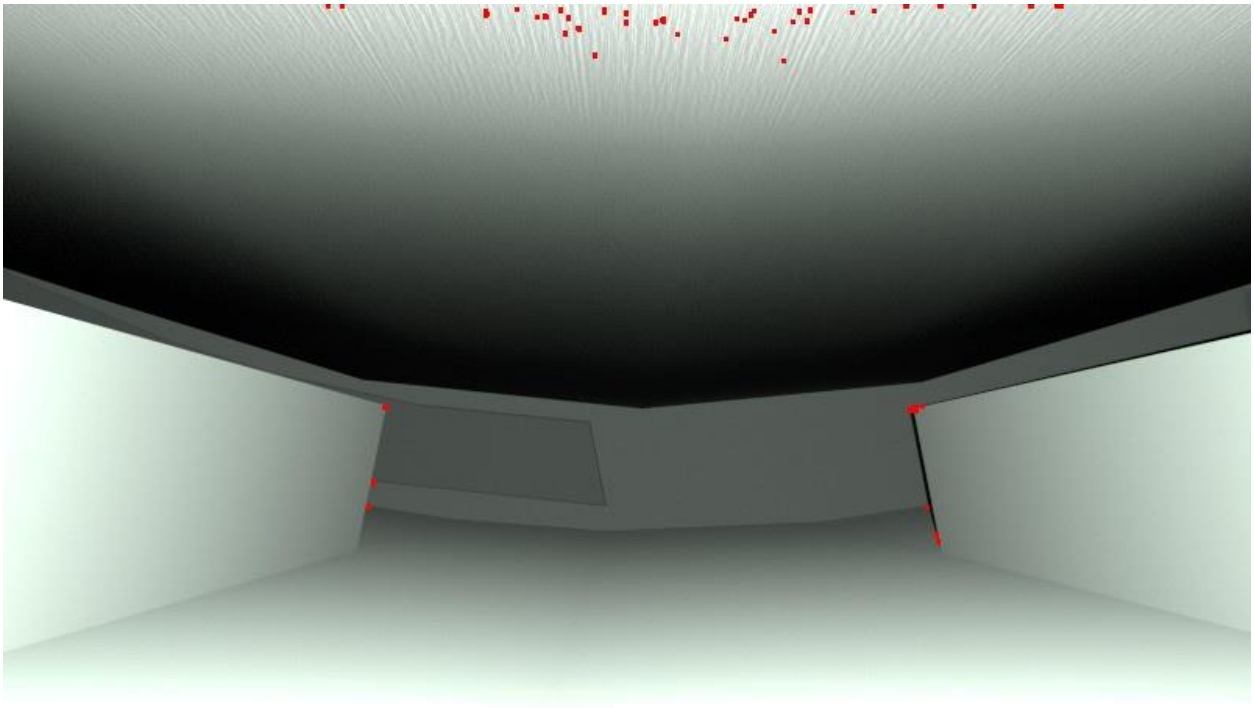

**Figure 21: Corner detection in complete simulation**

## Laser Separation

After moving to testing in the realistic simulation, we became aware of a technique used in ROVs for range finding [24]. By simply aiming two lasers at a distant surface, the apparent separation of their resulting reflections in the camera image can be used to infer range. As shown in Figure 22, we are easily able to pick out these points by using color thresholding.

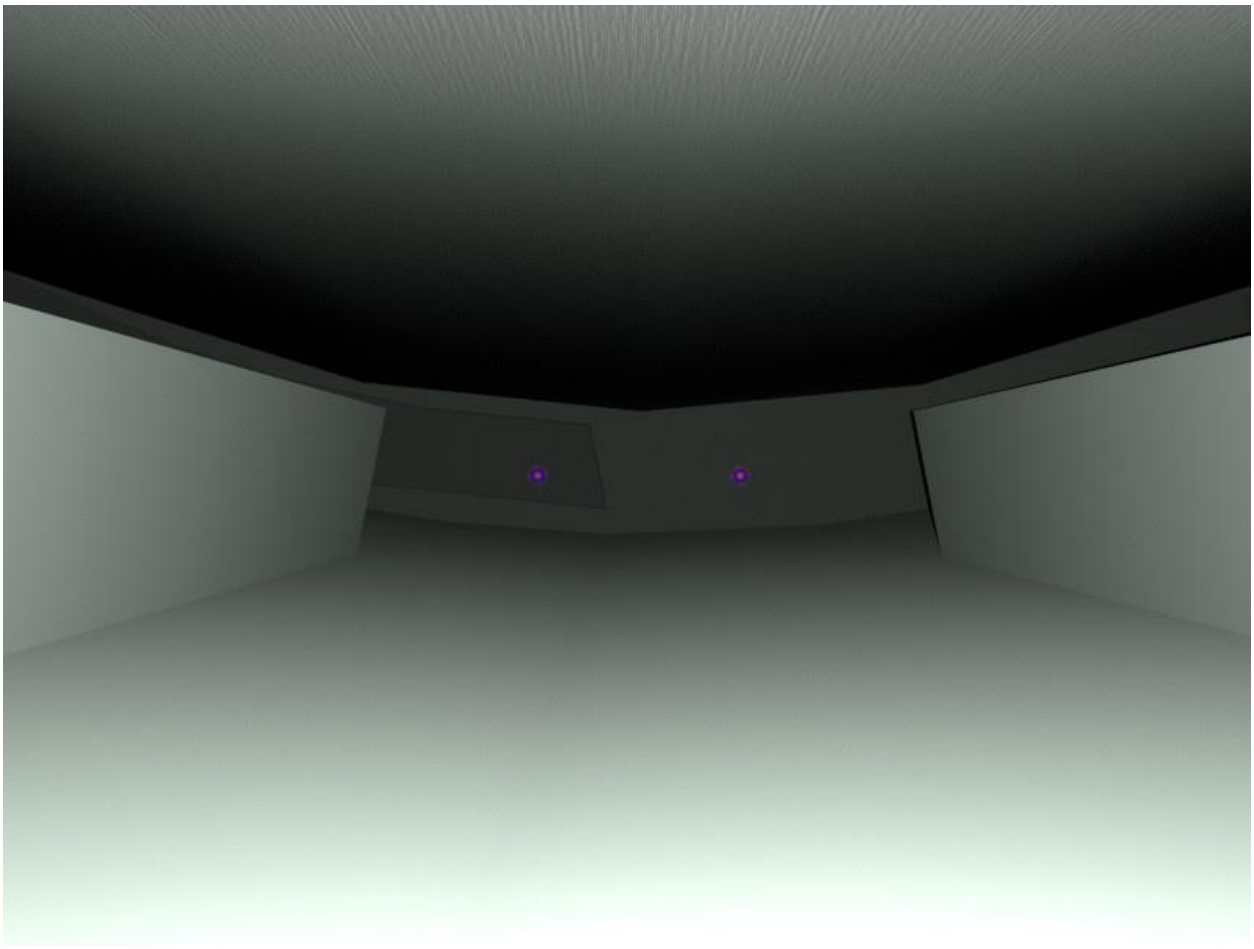

**Figure 22: Two blue circles mark the detected reflections from two laser pointers**

**Edge Detection**

While the corners within the realistic simulation are less apparent, the lines formed at the edges of the channel remain very visible. This inspired us to attempt to use them as a feature for localization. Due to the right-angle geometry, if we can detect these edges and fit lines to them, we can infer the coordinates of the corners by finding the intersections of the line segments. To extract these line segments, we apply a Canny edge filter and a probabilistic Hough transform. Using our prior knowledge that there should be a total of four lines in the image whose intersections give two points, we split the image vertically at the center, and process each half separately. We use K-means to cluster the many short segments given by the Hough transform into two lines, based on slope and intercept. We then equate these two lines to find their intersection, giving us the resultant image shown in Figure 23.

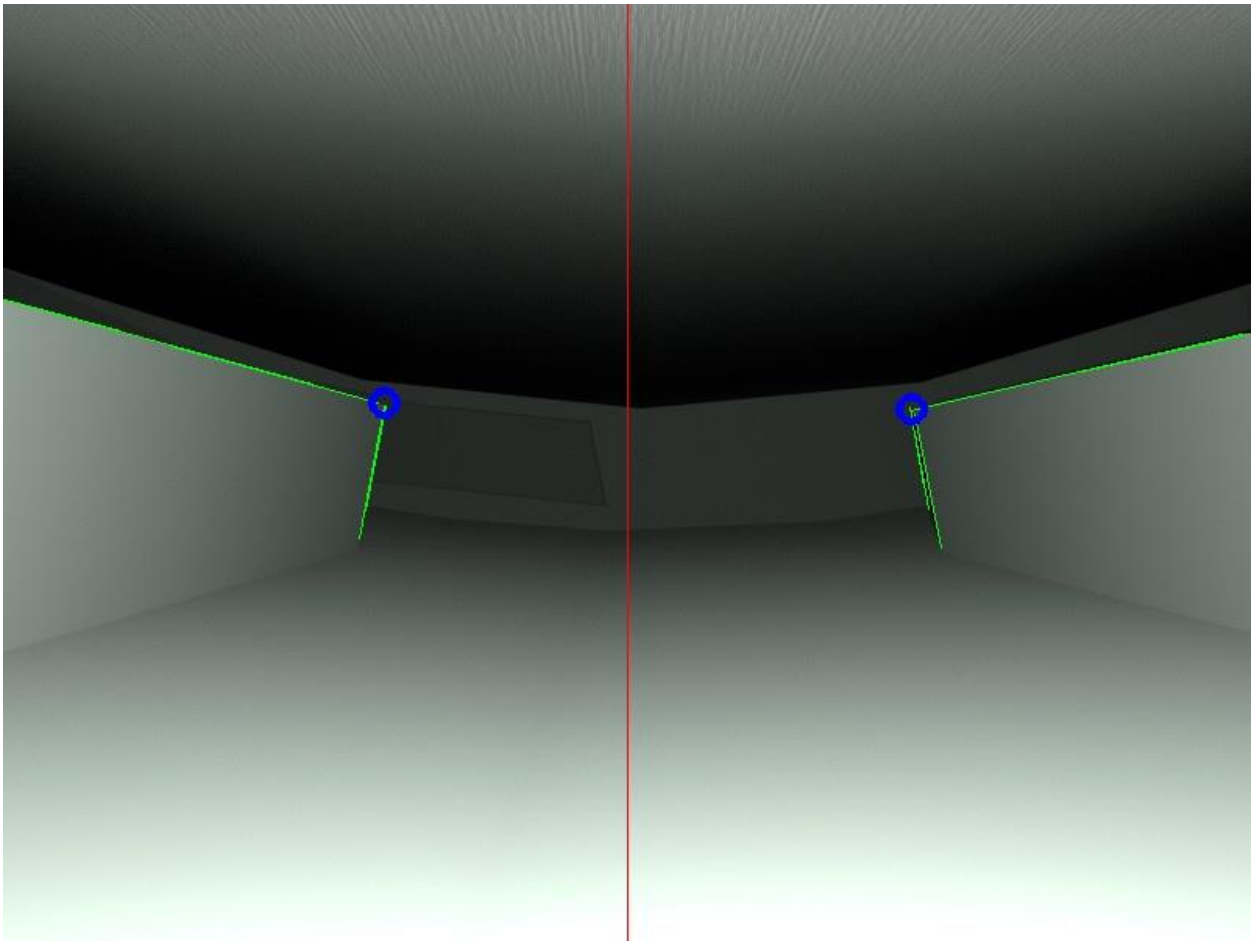

**Figure 23: Two blue circles highlight the identified intersections, green lines show the extracted edges, and a red line shows where the image is split into left and right halves**

# Chapter 5

## Physical Implementation and Testing

Based on the results of testing in the simulated environment, we chose to move forward to physical testing with the laser separation and line fitting techniques. These techniques showed promising results in simulation, and required a minimum of hardware to test.

### Mockup Cask

In order to more closely simulate the appearance of the interior of a DCSS than is possible with software, we designed and constructed a mockup of the channel section. Our mock-up consists of two parts: an upper element which simulates the MPC, and a lower element which simulates the overpack. The lower element is coated with a matte paint of similar characteristics to that used on the overpack, and the upper element is clad in a thin sheet of aluminum, to emulate the polished metal nature of the MPC. These two parts are separated by studs which can be adjusted to alter the standoff distance (Figure 24 and Figure 25).

**Figure 24: Upper and lower elements of the cask mockup**

**Figure 25: Cask mockup assembled**

## Robot Hardware

To test these techniques, we used a prototype robot inspection car named “Splinter”. Splinter is equipped with two PointGrey BlackFly cameras, a 1.5W LED lamp, and two 5mW lasers, as shown in Figure 26. For testing, we advanced Splinter through our mockup (Figure 27) and captured stills from the left camera, while recording the distance to the end plate of the mockup for use as ground truth.

**Figure 26: Inspection robot prototype “Splinter” with LED lamp and lasers**

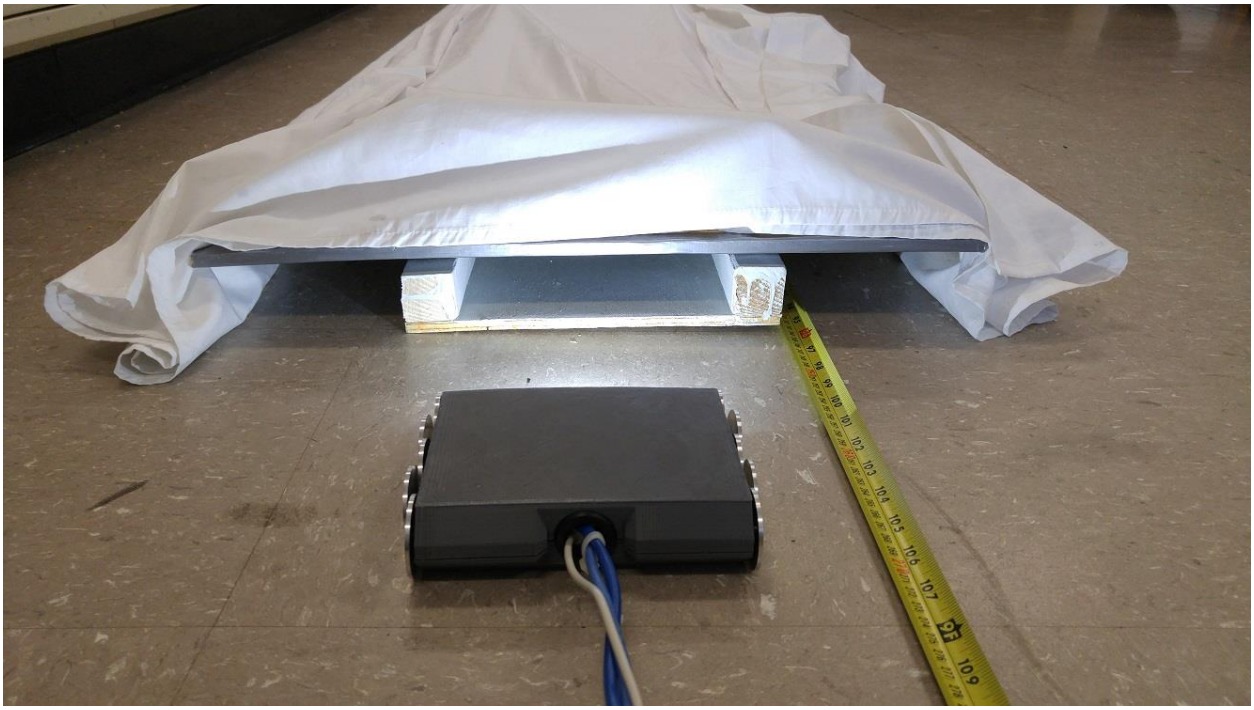

**Figure 27: Robot prototype at entrance to mockup (cloth in place to block ambient light)**

# Chapter 6

# Results

## Laser Separation

Measurement of laser separation performed well in the mockup, after tuning the parameters used for segmentation. However, the experiments revealed a few unexpected complications that were not predicted from simulation. First, the lasers in the mockup reflected off the MPC surface, creating several reflections. By noting that the "true" set of laser points appear largest and lowest in the image, it becomes easy to reject these reflections. The second issue was that the center of the laser points appear white in the camera surrounded by a red ring, due to their high intensity. By searching for this red ring instead of a solid blob, it was possible to view the laser points on a camera.

In our experiment, we captured stills at five positions within the mockup, and applied our algorithms to them offline. A representative image from this data set is shown in Figure 28, the calibration curve applied to find the relationship between laser separation and range is shown in Figure 29 (n = 5). This calibration was then tested on a separate data set (n = 20) to determine the measurement performance. After removing two outliers, the errors associated with this test were calculated and are shown in Figure 30 and Figure 31, where they exhibit an RMS value of

13.5cm and a standard deviation of 13.6cm. Note that the data set used for calibration covers a narrower range than the set used for evaluation, and the error shown in Figure 30 exhibits a positive trend with range. This strongly indicates that our calibration needs adjustment, and we may see decreased error with the application of a wider range of calibration values.

**Figure 28: View from the robot inside the mockup, the green line illustrates the distance used to measure laser separation**

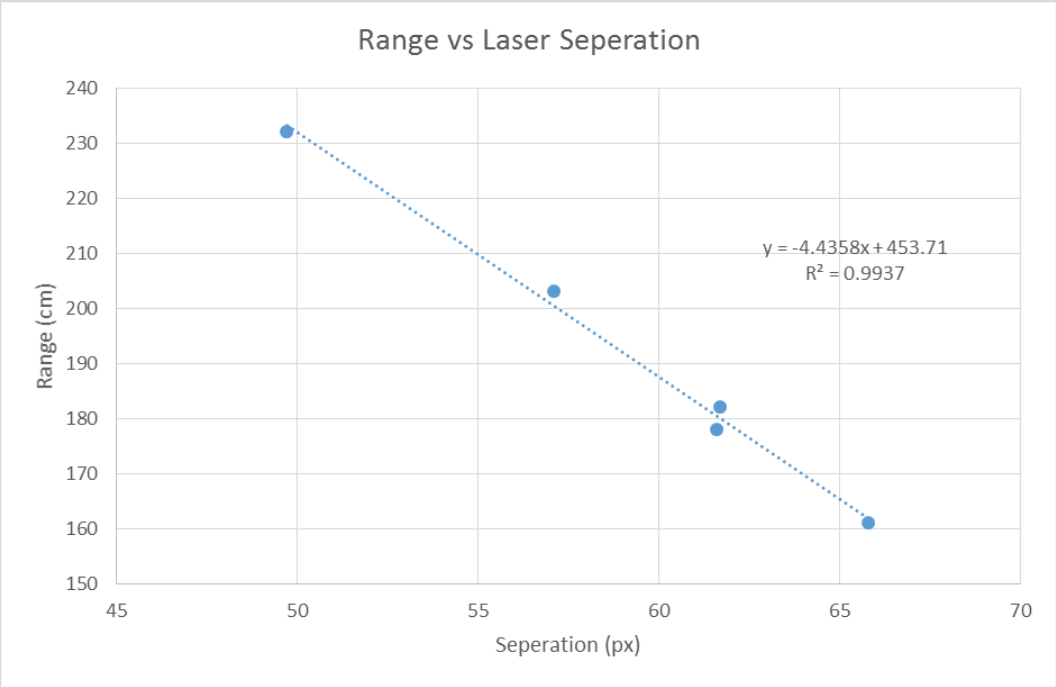


**Figure 29: Calibration curve of the relationship between laser separation and range**

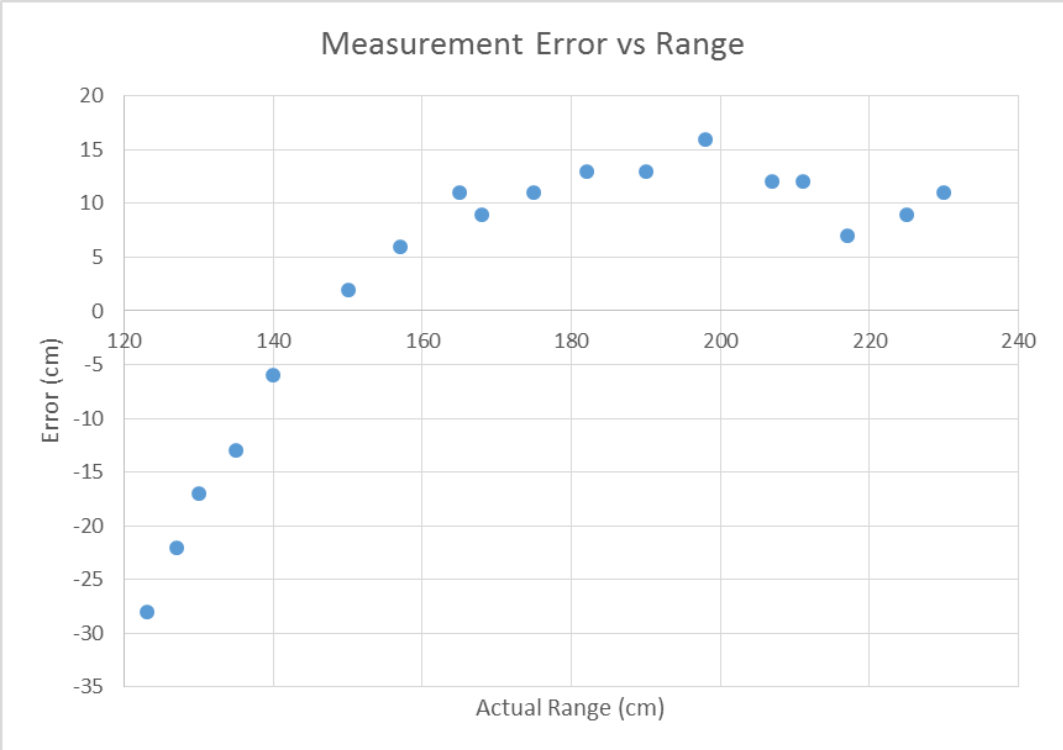


**Figure 30: The measurement error associated with application of the curve in Figure 29**

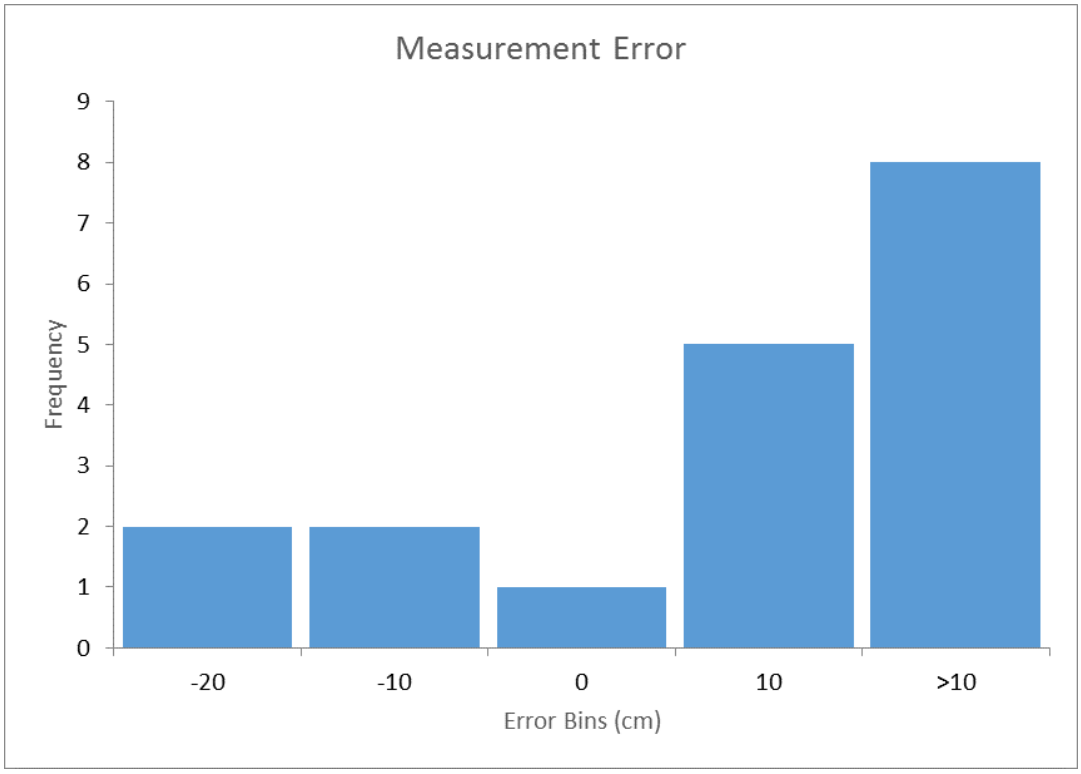


**Figure 31: Histogram showing the distribution of error values in Figure 30**

## Edge Detection

Unfortunately, edge detection in the mockup performed quite poorly. As can be observed in Figure 28, the lamp mounted on the robot had far less penetration than expected from simulation, and as a result, the edges of the guides are not discernable. By using different illumination and imaging hardware, we were able to obtain the image presented in Figure 32, which shows the edges of the guides quite clearly. However, we were unable to position this setup deep enough within the mockup to image the end plate, as required for this technique to be successful.

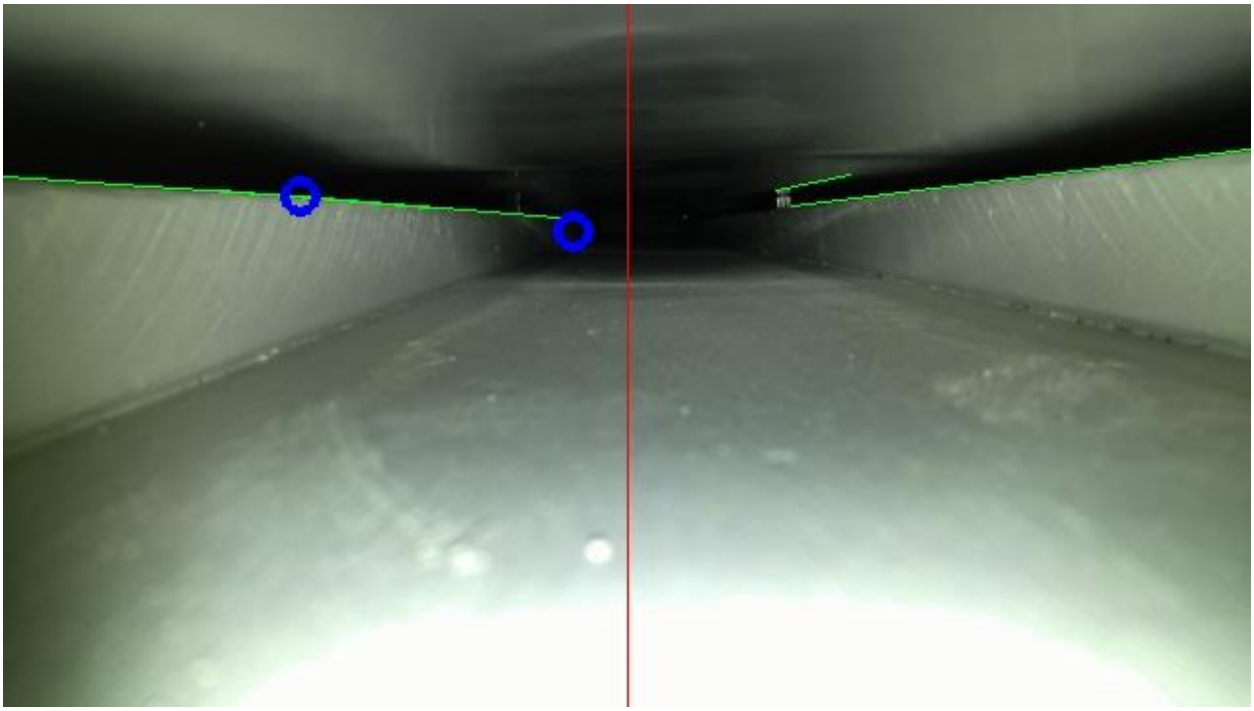

**Figure 32: Edge detection as applied to an image captured by secondary test equipment inside the mockup (for an explanation of the annotations, see Figure 23)**

# Chapter 7

## Conclusions

This thesis investigated various methods to localize an inspection robot inside a nuclear storage cask, testing several both in a virtual simulation and in a physical mockup of the cask. Of all the techniques explored, ranging via observation of the separation of lasers and edge detection within the environment performed the best in practice. The laser separation technique performed as expected, but does require that the inspection robot carry the lasers. This is undesirable as space is at a premium and more components will require additional cooling. The edge detection technique was unable to find edges in the image when used with the lamp currently installed on our robot prototype, but worked properly with more intense illumination. This technique would be preferable for deployment, as it does not require any additional hardware beyond what the robot has already been designed for.

Further work will focus on real-time implementation of these algorithms, and integration into ROS to operate alongside the other software required for the inspection robot. In addition, to take full advantage of the planned odometry readings, methods of data fusion should be explored to find the most accurate and precise estimates of robot position by combining the different modes of measurement.

# BIBLIOGRAPHY

[1] Nuclear Regulatory Commission, "Backgrounder on Radioactive Waste," 2015.

[2] J. J. Fialka, "The 'screw Nevada bill' and how it stymied U.S. nuclear waste policy," *The New York Times,* 11 May 2009.

[3] J. Lambert, S. Bakhtiari, I. Bodnar, C. Kot and J. Pence, "NRC Job Code V6060: Extended In-Situ and Real Time Monitoring Task 3: Long-Term Dry Cask Storage of Spent Nuclear Fuel," Argonne National Laboratory, Chicago, 2012.

[4] Holtec International, "Final Safety Analysis Report for the HI-STORM 100 Cask System," Holtec International, Marlton, New Jersey, 2010.

[5] R. Meyer, A. Pardini, J. Cuta, H. Adkins, A. Casella, A. Qiao, M. Larche, A. Diaz and S. Doctor, "NDE to Manage Atmospheric SCC in Canisters for Dry Storage of Spent Fuel: An Assessment," Pacific Northwest National Laboratory, Richland, 2013.

[6] D. Filmore, Literature Review of the Effects of Radiation and Temperature on the Aging of Concrete, United States. Department of Energy, 2004.

[7] F. Glasser, J. Marchand and E. Samson, "Durability of concrete — Degradation phenomena involving detrimental chemical reactions," *Cement and Concrete Research*, vol. 38, no. 2, pp. 226-246, 2008.

[8] Nuclear Regulatory Commission, "Premature degradation of spent fuel storage cask structures and components from environmental moisture," Washington, 2013.

[9] S. Bakhtiari, T. Elmer, E. Koehl, K. Wang, A. Raptis, D. Kunerth and S. Birk, "Dry Cask Storage Inspection and Monitoring. Interim Report.," Argonne National Laboratory, Argonne, 2014.

[10] C. Lissenden, A. Motta, I. Jovanovic, S. Brennan, K. Reichard, J. Popovics and T. Knight, *Technical Proposal: Multi-Sensor Inspection and Robotic Systems for Dry Storage Casks*, 2014.

[11] S. Brennan, K. Reichard, B. Leary and B. McNelly, "NEUP - Nuclear Inpection Robot," The Pennsylvania State University, University Park, 2015.

[12] F. Tache, F. Pomerleau, G. Caprari, R. Siegwart, M. Bosse and R. Moser, "Three-dimensional localization for the MagneBike inspection robot," *Journal of Field Robotics*, vol. 28, no. 2, pp. 180-203, 2011.

[13] A. Ahrary, Y. Kawamura and M. Ishikawa, "A laser scanner for landmark detection with the sewer inspection robot KANTARO," in *2006 IEEE/SMC International Conference on System of Systems Engineering*, 2006.

[14] A. Nassiraei, Y. Kawamura, A. Ahrary, Y. Mikuriya and K. Ishii, "Concept and Design of A Fully Autonomous Sewer Pipe Inspection Mobile Robot "KANTARO"," in *2007 IEEE International Conference on Robotics and Automation*, 2007.

[15] A. Morris, D. Ferguson, Z. Omohundro, D. Bradley, D. Silver, C. Baker, S. Thayer, C. Whittaker and W. Whittaker, "Recent developments in subterranean robotics," *Journal of Field Robotics,* vol. 23, no. 1, pp. 35-57, 2006.

[16] A. Markham, N. Trigoni, D. Macdonald and S. Ellwood, "Underground Localization in 3-D Using Magneto-Inductive Tracking," *IEEE Sensors Journal,* vol. 12, no. 6, pp. 1809-1816, 2012.

[17] H. Qi, X. Zhang, H. Chen and J. Ye, "Tracing and localization system for pipeline robot," *Mechatronics,* vol. 19, no. 1, pp. 76-84, 2009.

[18] K. Konolige, "Projected texture stereo," in *2010 IEEE International Conference on Robotics and Automation (ICRA)*, 2010.

[19] A. Leeper, K. Hsiao, E. Chu, J. K. Salisbury, O. Khatib and G. Sukhatme, "Using Near-Field Stereo Vision for Robotic Grasping in Cluttered Environments," in *Experimental Robotics*, Springer Berlin Heidelberg, 2014, pp. 253-267.

[20] G. Zhang, J. He and X. Li, "3D vision inspection for internal surface based on circle structured light," *Sensors and Actuators A: Physical,* vol. 122, no. 1, pp. 68-75, 2005.

[21] D. Martin, "A practical guide to machine vision lighting," October 2007. [Online]. Available: http://www.graftek.com/pdf/Marketing/MachineVisionLighting.pdf. [Accessed 29 September 2015].

[22] P. Hansen, H. Alismail, P. Rander and B. Browning, "Monocular visual odometry for robot localization in LNG pipes," in *2011 IEEE International Conference on Robotics and Automation (ICRA)*, 2011.

[23] J. Z. De Paz, E. C. Castaneda, X. S. Castro and S. R. Jimenez, "Crack detection by a climbing robot using image analysis," in *2013 International Conference on Electronics, Communications and Computing (CONIELECOMP)*, 2013.

[24] G. Karras, D. Panagou and K. Kyriakopoulos, "Target-referenced Localization of an Underwater Vehicle using a Laser-based Vision System," in *OCEANS 2006*, 2006.

# ACADEMIC VITA

**Academic Vita of Jacob Beck**
Jzb220@psu.edu

## Education

B.S. in Mechanical Engineering

Honors student of the Schreyer Honors College

## Thesis Title

A Combined Approach to Localization for a Nuclear Cask Inspection Robot

## Thesis Supervisor

Sean Brennan, Associate Professor of Mechanical Engineering

## Work Experience

January to April, 2015 - NASA LaRC Autonomy Incubator

Robotics Intern - Developed robotics control software and gripping technology

Supervised by James Neilan

May to July, 2014 – Penn State Ultrasonic Transducers Lab

Undergraduate Researcher - Researched and developed dry-coupled magnetostrictive transducers

Supervised by Prof. Cliff Lissenden

**Grants Received**

Crowley Jr. Memorial scholarship

Hand Honors scholarship

**Awards**

Honors certificate in STEM

2nd place at CodePSU

**Publications:**

"Dry coupled magnetostrictive transducers for robotic inspection of dry storage casks" – Poster at WMS2015

**International Education:**

Spring 2015 - Study abroad at Tohoku University, Sendai, Japan